Parametric frequency conversion in photonic crystal fibres with germanosilicate core

2007 J. Opt. A: Pure Appl. Opt. 9 716

(http://iopscience.iop.org/1464-4258/9/7/025)

J. Opt. A: Pure Appl. Opt. **9** (2007) 716–722 doi:10.1088/1464-4258/9/7/025

Parametric frequency conversion in photonic crystal fibres with germanosilicate core

Yu P Yatsenko and A D Pryamikov

Fiber Optics Research Center of the Russian Academy of Sciences, 38 Vavilov Street, 119991 Moscow, Russia

E-mail: yuriya@fo.gpi.ru (Yu P Yatsenko)

Received 16 April 2007, accepted for publication 31 May 2007
Published 20 June 2007
Online at stacks.iop.org/JOptA/9/716

Abstract
Numerical analysis of dispersion and nonlinear characteristics of photonic crystal fibres (PCFs) with a small number of hole rings and large (>20 mol%) concentrations of GeO_2 in the core is performed. It is shown that by proper choice of the fibre design and, in particular, the diameter of a doped core and the GeO_2 concentration, it is possible to obtain a high nonlinearity coefficient simultaneously with the desired dispersion characteristic and to realize efficient parametric frequency conversion with large Stokes shifts at a pump in the vicinity of 1.1 μm.

Keywords: photonic crystal fibres, dispersion, nonlinearity coefficient, parametric frequency conversion

1. Introduction

A remarkable variety of dispersion characteristics was demonstrated lately in silica photonic crystal fibres (PCFs) [1–7]. By changing the air hole structure, it is possible to shift the zero dispersion wavelength up to the green region [2, 3], to obtain the ultra-flattened nearly-zero dispersion over a wide wavelength range around 1.5 μm [4–6] and to form the dispersion shape with two or more zeros [6, 7]. Unique properties of silica PCFs often allow the desired dispersion shape to be achieved simultaneously with a small effective mode area and, correspondingly, a large nonlinear coefficient $\gamma = 2\pi n_2/(\lambda A_{\mathrm{eff}})$ (n_2 is the nonlinear refractive index, λ is the wavelength and A_{eff} is the effective mode area). Thus, γ values of about 95 $(\mathrm{W\,km})^{-1}$ were obtained in the vicinity of the zero dispersion wavelength at 750 nm in the silica PCF [8]. Such nonlinear coefficients make it possible to use short fibre lengths of a few tens of metres for parametric frequency conversion and amplification of optical signals. At these fibre lengths, it is much easier to obtain a high optical quality, which is necessary to satisfy strict phasematching condition for a four-wave mixing (FWM) process. In particular, the most dangerous long-period fluctuations of fibre parameters along the fibre can be avoided [9]. However, achieving large γ values at zero dispersion wavelengths longer than 1 μm remains difficult in pure silica PCFs. This comes from the need for an increase in the hole-to-hole spacing or a decrease in the hole diameters to obtain the zero dispersion at longer wavelengths. Such structure changes are accompanied by an increase in the effective mode area [10].

It has been shown recently that PCFs with a germanosilicate core are very promising for obtaining the desired dispersion curve, while keeping a small effective mode area [11]. On the one hand, the GeO_2 dopant is known to enhance nonlinear properties of silica and, on the other, it shifts the zero dispersion to the long-wavelength region not so significantly as compared to lead silicate and tellurite fibres. In the latter fibres with much higher nonlinear coefficients, it is difficult to achieve the shift of the zero dispersion wavelength to the region shorter than 1.5 μm. In [11], fibres had 12 rings of air holes and a germanium-doped core region. An increase in the nonlinear coefficient of up to 11.2 $(\mathrm{W\,km})^{-1}$ at a very low dispersion slope of 0.001 ps nm^{-2} km^{-1} at 1.55 μm was shown to be possible with this fibre design.

In this paper, we made numerical modelling of the dispersion and nonlinear characteristics of the PCFs containing only 2–4 rings of holes and large (>20 mol%) GeO_2 concentrations in the core. Our analysis of the dispersion

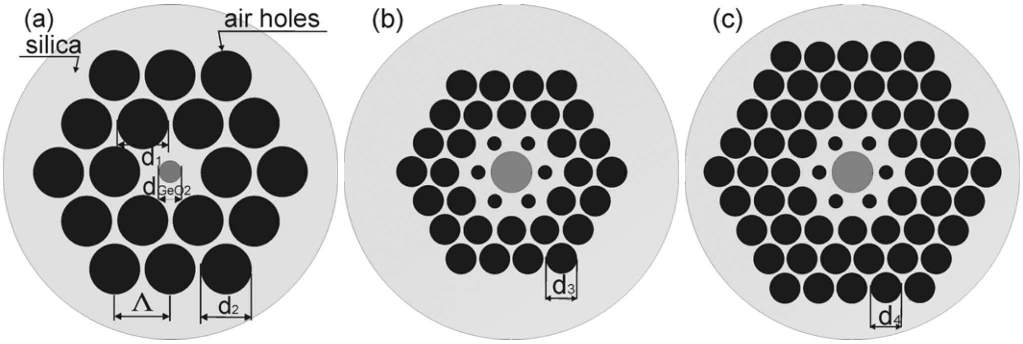

Figure 1. The cross sections of the studied fibres: (a) with two rings of holes ($d_1/\Lambda = d_2/\Lambda = 0.9$); (b) with three rings of holes ($d_3/\Lambda = 0.9$); (a) with four rings of holes ($d_3/\Lambda = d_4/\Lambda = 0.9$).

and nonlinear characteristics was applied to obtain FWM with Stokes shifts of 2000–3000 cm^{-1} at a pump in the region of 1.1 μm. A fibre converter with such large frequency shifts makes it possible to realize frequency conversion between telecommunication bands at 0.85 μm and at 1.3 or 1.5 μm. It was shown that by properly choosing the diameter of a doped core and the GeO_2 concentration, it is possible to obtain a high nonlinearity coefficient simultaneously with a desired dispersion characteristic and to realize efficient parametric frequency conversion in this wavelength region.

2. Analysis method

A precise control of dispersion and waveguide characteristics is necessary to make the FWM process with large Stokes shifts effective. With single-mode PCFs, it became possible. To illustrate this, we consider the well-known relations of the FWM process [12]. The conversion efficiency at the Stokes wavelength, neglecting pump depletion and losses, is written as

$$G = \frac{P_s(L)}{P_a(0)} = \left(1 + \left(\frac{\Delta k_1}{2g}\right)^2\right)\sinh^2(gL) \tag{1}$$

where

$$g = \sqrt{(\gamma P_p)^2 - \left(\frac{\Delta k_1}{2}\right)^2} \tag{2}$$

$$\Delta k_1 = \Delta k + 2\gamma P_p. \tag{3}$$

P_p is the pump power at the frequency ω_p; P_a, P_s are the signal powers at the anti-Stokes frequency ω_a and at the converted Stokes frequency $\omega_s = 2\omega_p - \omega_a$, respectively; L is the fibre length.

The difference of the propagation constants of the interacting waves is $\Delta k = \beta_a + \beta_s - 2\beta_p$, where β_a, β_s and β_p are the propagation constants of the anti-Stokes, the Stokes and the pump waves, respectively, and the nonlinear term $2\gamma P_p$ contributes to the phase mismatch Δk_1.

Expanding $\Delta k = \beta_a + \beta_s - 2\beta_p$ in Tailor's series near the pump frequency yields

$$\Delta k = 2\sum_{m=1}^{\infty} \beta_{2m} \frac{(\omega_s - \omega_p)^{2m}}{(2m)!} \tag{4}$$

where $\beta_{2m} = \frac{d^{2m}k}{d\omega^{2m}}|_{\omega_p}$ are the $2m$-order dispersion coefficients at the pump frequency.

The phasematching of wavevectors $\Delta k_1 = 0$ is necessary to maximize the amplification coefficient g. From (3), we should have $\Delta k < 0$. For not too large Stokes shifts, we can use only the first term in (4), which depends on the second-order dispersion β_2. It can be represented near zero dispersion wavelength λ_0 as

$$\Delta k = -\frac{2\pi c}{\lambda_p^2}\frac{dD}{d\lambda}\bigg|_{\lambda_0}(\lambda_p - \lambda_0)(\lambda_s - \lambda_p)^2 \tag{5}$$

where $D = -(2\pi c/\lambda^2)\beta_2$, and λ_p and λ_s are the pump and the Stokes wavelengths, respectively.

As follows from (5), the phasematching is possible only in the region of anomalous dispersion $\beta_2 < 0$, where $\lambda_p > \lambda_0$. Close to the second-order dispersion zero, it is fully defined by the nonlinear term $2\gamma P_p$. But for large frequency shifts $(\omega_s - \omega_p)$, the phase mismatch Δk in (5) becomes too large even at a small displacement of the pump wavelength from the zero wavelength to be compensated by a nonlinear term $2\gamma P_p$. However, considering the contribution of the higher dispersion terms in (4), which have different signs, it can be shown [13] that the pump wavelengths, for which the phasematching condition is satisfied, exist in the normal dispersion region. Here, the phasematching condition is defined mainly by the fibre dispersion characteristics and weakly depends on $2\gamma P_p$ ($\Delta k_1 \approx \Delta k = 0$). This affords tuning the phasematched Stokes frequencies by shifting the pump wavelength to the left from the dispersion zero. In single-mode fibres, this tuning band is close to the zero dispersion wavelength and is rather narrow, a few tens of nanometres. Therefore, in the PCFs, which permit shifting the dispersion zero to the short wavelength band, the phasematching is possible for pumps in the region of 1.1 μm [13]. Moreover, the PCFs allow obtaining the dispersion shape with two zeros in the wavelength range 0.8–1.5 μm. The wavelength region between two zeros belongs to the anomalous dispersion region and can be varied over hundreds of nanometres by changing the fibre parameters. As shown in [8], the phasematching for large Stokes shifts with a weak dependence on $2\gamma P_p$ is also possible in this region.

We studied two types of PCFs with a germanosilicate core shown in figure 1.

The first one had two rings of the holes with a large ratio of the hole diameter d to the pitch Λ, $d/\Lambda = 0.9$ (figure 1(a)). For this fibre, our analysis was made for two GeO_2 concentrations in the core, 24 and 50 mol%.

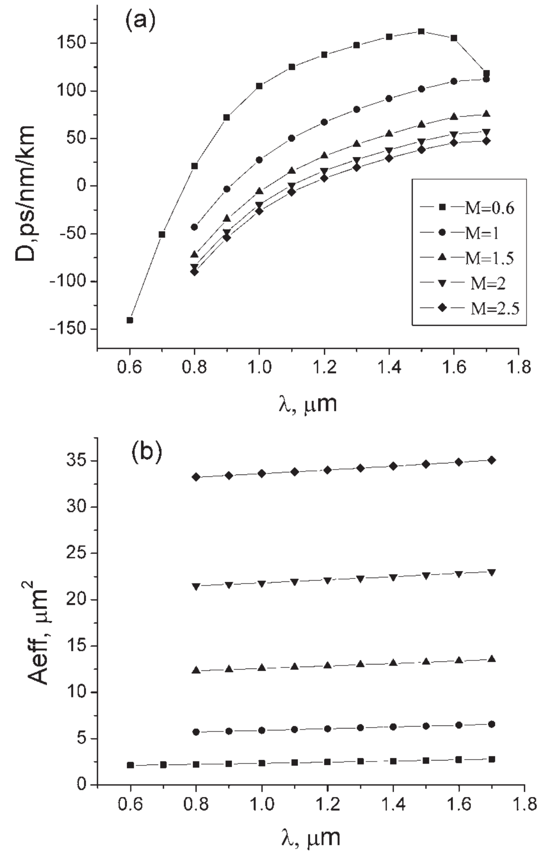

Figure 2. The dispersion (a) and the effective mode area (b) as functions of the wavelength at different scaling coefficients M in a two-ring fibre with the silica core. $M = 1$: $d/\Lambda = 0.9$ and $\Lambda = 3.1\ \mu$m.

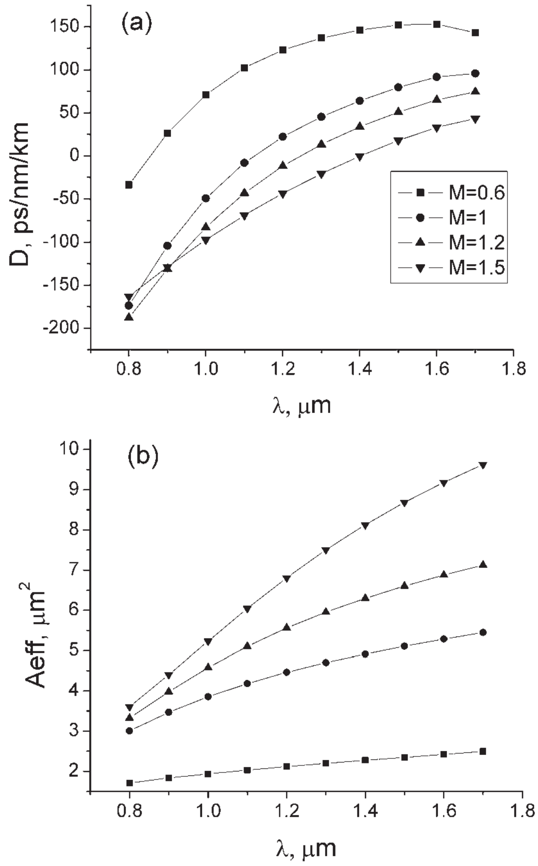

Figure 3. The dispersion (a) and the effective mode area (b) as functions of the wavelength at different scaling coefficients M in a two-ring fibre with the 24 mol% GeO_2-doped core. $M = 1$: $d/\Lambda = 0.9$, $\Lambda = 3.1\ \mu$m, and $d_{GeO_2} = 1.2\ \mu$m.

The structure of the second type, shown in figures 1(b) and (c), consisted of 3–4 hole rings and the core doped with 24 mol% GeO_2. For the first two inner rings, the value of d/Λ could be changed. For the third and the fourth outer rings, it was unchangeable: $d_3/\Lambda = d_4/\Lambda = 0.9$.

The calculation of dispersion characteristics was made by the finite element method, using the commercial Matlab–Femlab package. The perfectly matched layers were inserted for the evaluation of the confinement loss [7, 14]. For optimization of the dispersion characteristics in the PCFs with different d/Λ in the rings, we applied a Genetic Algorithm (GA) [18, 19]. The variation parameters were the diameter of the germanosilicate core d_{GeO_2}, the hole diameters in the first two rings d_1, d_2 and the pitch Λ. The dispersion shape was optimized, taking into account the magnitude of the phasematched Stokes shifts, which can be obtained with this shape. As a rule, the initial population of ten individuals and 15–16 generations were employed to obtain the desirable dispersion profile. For calculation of the Stokes shifts, which satisfy the phasematching condition (3), we used the higher-order dispersion terms, up to eighth order in expansion (4).

3. PCFs with one dispersion zero

The obvious advantage of PCFs with a large d/Λ is a low confinement loss at a small number of rings. In a fibre with the two rings of holes in hexagonal symmetry, the confinement loss is less than 1 dB km^{-1} in the wavelength range 0.8–1.6 μm [15]. The smallest effective mode area can be achieved also with these fibres, as they potentially have the largest effective refractive index and the smallest core diameter ($d_{core} = \Lambda(2-d/\Lambda)$). With $d/\Lambda \geqslant 0.9$, broad control of dispersion is possible only through scaling (a proportional change of d_{core}, d and Λ with d/Λ being unchanged), and obtaining a complicated shape of the dispersion curve is difficult. Nevertheless, by scaling, the dispersion with a single zero in the region of 1.1 μm is easy to obtain.

Figures 2 and 3 show the dispersion curves and the effective mode area at different values of scaling parameter M (the coefficient of the proportional change of the original structure for which $M = 1$), calculated for the two-ring PCFs with $d/\Lambda = 0.9$ in both rings. The dispersion characteristic of the pure silica PCF, shown in figure 2(a), experiences an essential shift towards the long-wavelength region only at a significant increase of the scaling parameter M. At $M = 0.6$, the effective mode area is $A_{eff} = 2.2\ \mu m^2$ and the nonlinear coefficient is $\gamma = 77$ (W km)$^{-1}$ at the zero wavelength $\lambda_0 = 0.77\ \mu$m, taking the nonlinear refractive index for silica $n_2 = 2.16 \times 10^{-16}$ cm^2 W^{-1} [16]. The zero wavelength is close to 1.1 μm at $M = 2$, where $A_{eff} = 22\ \mu m^2$ and $\gamma = 5.6$ (W km)$^{-1}$. Thus, a three-to fourfold increase of M

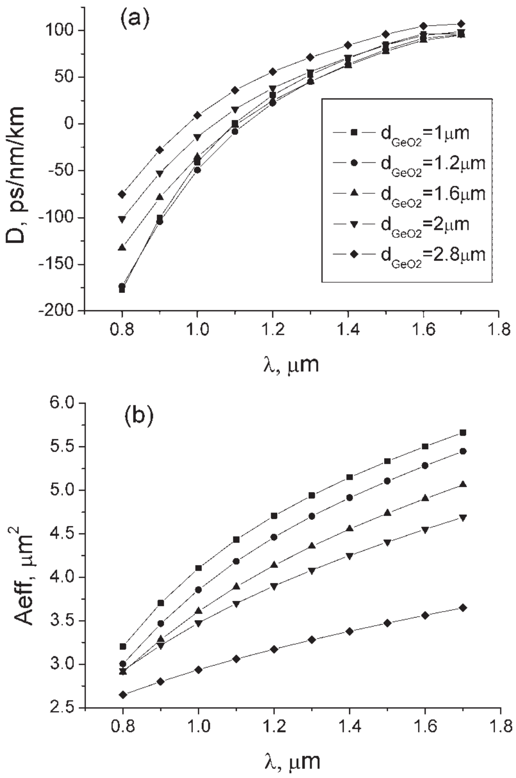

Figure 4. The dispersion (a) and the effective area (b) as functions of the wavelength at different diameters $d_{\mathrm{GeO_2}}$ of the 24 mol% $\mathrm{GeO_2}$-doped core, $\Lambda = 3.1$ μm, and $d/\Lambda = 0.9$.

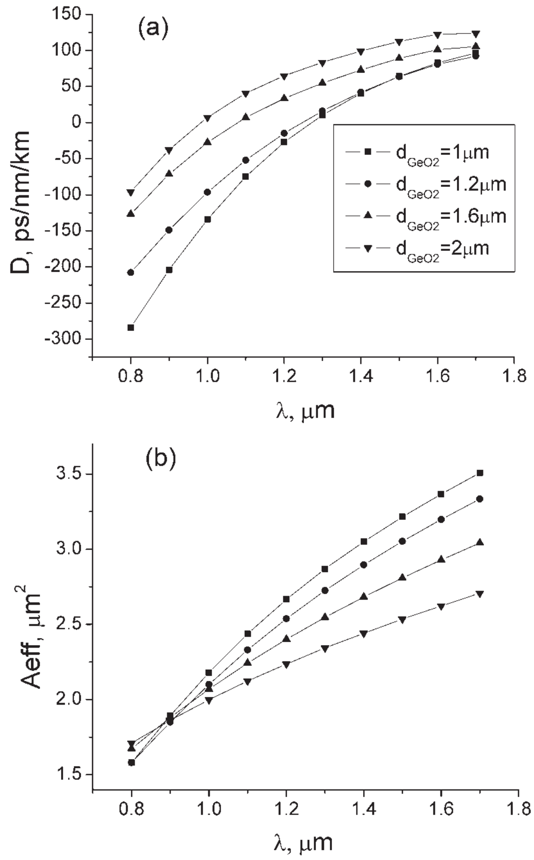

Figure 5. The dispersion (a) and the effective area (b) as functions of the wavelength at different diameters $d_{\mathrm{GeO_2}}$ of the 50 mol% $\mathrm{GeO_2}$-doped core, $\Lambda = 2.48$ μm, and $d/\Lambda = 0.9$.

is necessary to shift the zero wavelength from the region 0.8 to 1.1 μm. Such an increase is accompanied by increasing the effective mode area and accordingly by decreasing the nonlinear coefficient by more than one order of magnitude.

Contrary to that, as was shown in figure 3, for a PCF with the 24 mol% $\mathrm{GeO_2}$-doped core, having the ratio of the doped part to the core diameter $d_{\mathrm{GeO_2}}/d_{\mathrm{core}} = 0.35$, the dispersion zero shifts to the 1.1 μm region already at $M = 1$. The effective mode area is 4.2 $\mu\mathrm{m}^2$ and $\gamma = 40$ $(\mathrm{W\,km})^{-1}$ at 1.1 μm. While evaluating γ, we took $n_2 = 2.95 \times 10^{-16}$ $\mathrm{cm^2\,W^{-1}}$, using its empirical dependence on $\mathrm{GeO_2}$ concentration, given in [16]. Hence, at this zero dispersion wavelength, the nonlinear coefficient in the PCF with the 24 mol% $\mathrm{GeO_2}$-doped core is seven times higher than in the PCF with the silica core.

Figures 4 and 5 demonstrate how dispersion and mode field characteristics change with the diameter of a doped core $d_{\mathrm{GeO_2}}$ and with the $\mathrm{GeO_2}$ concentration. Increasing $d_{\mathrm{GeO_2}}$ at fixed Λ and d results in a shift of the dispersion first to a longer and then to a shorter wavelength region. Contrary to an influence on the dispersion slope of the scaling parameter shown in figures 2 and 3, the dispersion slope is defined mostly by changes in the short wavelength region at changing $d_{\mathrm{GeO_2}}/d_{\mathrm{core}}$. This follows from the competition between waveguiding properties, defined by the germanosilicate core and the geometry of holes. In the extreme cases, when $d_{\mathrm{GeO_2}}/d_{\mathrm{core}} \ll 1$ or $d_{\mathrm{GeO_2}}/d_{\mathrm{core}} \sim 1$, waveguiding properties are defined by the hole geometry, which manifests itself first of all in the longer wavelength region, where the mode field diameter is larger. For intermediate values of $d_{\mathrm{GeO_2}}/d_{\mathrm{core}}$, the largest changes are in the shorter wavelength region, where the germanosilicate core with a core–cladding refractive index difference $\Delta n = n_{\mathrm{SiO_2/GeO_2}} - n_{\mathrm{SiO_2}}$ localizes the fundamental mode well. Figure 4 shows that the influence of the doped core is maximum at $d_{\mathrm{GeO_2}} = 1.2$ μm for 24 mol% $\mathrm{GeO_2}$ and $\Lambda = 3.1$ μm. The shift of the dispersion zero to the longer wavelength region is the largest ($\lambda_0 = 1.1$ μm) and the nonlinear coefficient at 1.1 μm is the highest at these fibre parameters. With decreasing the pitch from the optimal value of $\Lambda = 3.1$, the dispersion curves with different $d_{\mathrm{GeO_2}}$ will have $\lambda_0 < 1.1$ μm, and with its increasing, the effective mode area will be larger.

As seen from figure 5, the dependence of the zero wavelength dispersion shift on the parameters Λ and $d_{\mathrm{GeO_2}}$ is even more sharp for 50 mol% $\mathrm{GeO_2}$ in the core. The same shift can be obtained here at smaller Λ and, respectively, a smaller effective mode area in comparison with 24 mol% $\mathrm{GeO_2}$ in the core. The dispersion zero is close to 1.1 μm at $\Lambda = 2.48$ μm and $d_{\mathrm{GeO_2}} = 1.6$ μm. The effective mode area at this wavelength is found to be $A_{\mathrm{eff}} = 2.24$ $\mu\mathrm{m}^2$ and the nonlinear coefficient is $\gamma = 97$ $(\mathrm{W\,km})^{-1}$, taking $n_2 = 3.81 \times 10^{-16}$ $\mathrm{cm^2\,W^{-1}}$ for this concentration.

As follows from the results, shown in figures 2–5, the $\mathrm{GeO_2}$ concentration and the $d_{\mathrm{GeO_2}}/d_{\mathrm{core}}$ ratio are additional structural parameters, allowing accurately tuning the dispersion zero, the dispersion slope and the effective mode area.

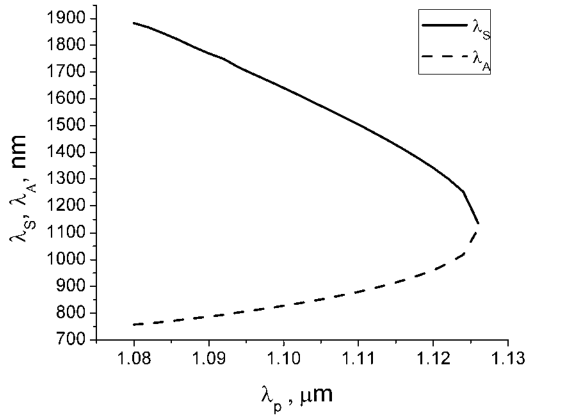

Figure 6. The phasematched wavelengths of a Stokes–anti-Stokes pair as functions of pump wavelength calculated for the two-ring fibre with the 24 mol% GeO_2-doped core, $d/\Lambda = 0.9$, $\Lambda = 3.1\ \mu$m, and $d_{GeO_2} = 1.2\ \mu$m.

Figure 6 shows the dependence of the phasematched Stokes–anti-Stokes wavelengths on the pump wavelength calculated for the fibre with 24 mol% GeO_2 in the core, $d_{GeO_2} = 1.2\ \mu$m and $\Lambda = 3.1\ \mu$m. At this phasematched diagram, the Stokes shift of 2632 cm^{-1} can be found at $\lambda_p = 1.106\ \mu$m, which makes the wavelength conversion from 857 to 1560 nm possible. For an ideal case of constant parameters along the fibre, the evaluation of FWM efficiency in accordance with (1)–(4) gives 10 dB amplification for the converted signal at the pump power of 1 W and the fibre length of 50 m.

4. PCFs with two dispersion zeros

For achieving efficient FWM with Stokes shifts of about 2000–3000 cm^{-1}, the PCFs with two dispersion zeros are very promising [8, 17]. Their main advantage is a low dispersion slope in a broad wavelength range which could make it easier achieving phasematching for large Stokes shifts. Such fibres have a more complicated structure, because they should have a larger number of rings with small and, as a rule, different values of d/Λ. By using GA, we analysed the simplest design of three-ring PCFs with variable d/Λ only in the first two rings.

Figure 7(a) shows how the dispersion characteristic with two zeros (curve (f1)) obtained in the PCF with 24 mol% GeO_2-doped core, $\Lambda = 1.35\ \mu$m, $d_{GeO_2} = 1.4\ \mu$m, $d_1/\Lambda = 0.46$, $d_2/\Lambda = 0.42$, and $d_3/\Lambda = 0.9$, changes with the diameter of the doped core d_{GeO_2} and with the scaling parameter M. With d_{GeO_2} varying, the dispersion curve varies without a noticeable shift of its maximum on the wavelength scale. With M varying, both the dispersion maximum and its position on the wavelength scale are changed. From figure 7(b), we see some relation between the dispersion changes and the calculated wavelengths for the phasematched Stokes–anti-Stokes pair. Contrary to the two-ring fibre considered above, the dispersion slope is lower in this PCF and approaches zero at the dispersion maximum. For such a specific dispersion shape, the phasematching for large Stokes shifts is possible for the pump wavelengths, positioned in the region of anomalous dispersion between the two zeros.

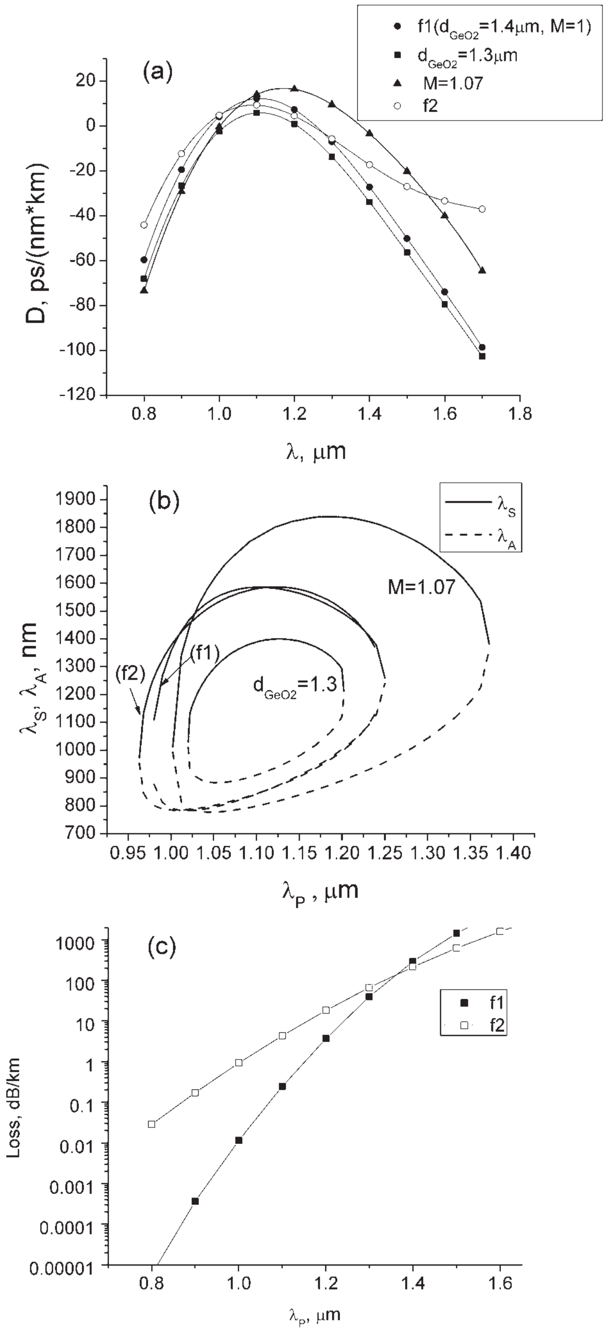

Figure 7. The dispersion (a), the phasematched Stokes–anti-Stokes wavelengths (b) and the confinement loss (c) as functions of the wavelength for the fibre (f1) with 24 mol% GeO_2-doped core, $\Lambda = 1.35\ \mu$m, $d_{GeO_2} = 1.4\ \mu$m, $d_1/\Lambda = 0.46$, $d_2/\Lambda = 0.42$ and $d_3/\Lambda = 0.9$, and for the pure silica fibre (f2) with $\Lambda = 1.74\ \mu$m, $d_1/\Lambda = 0.47$, $d_2/\Lambda = 0.22$ and $d_3/\Lambda = 0.9$. Influence of the parameters d_{GeO_2} and M on the dispersion and the phasematched Stokes–anti-Stokes wavelengths in fibre (f1) is also shown.

The dependence of the Stokes shifts on the pump wavelength has a maximum. Its value correlates with the value of the dispersion maximum and the wavelength interval between two zeros. Obviously, the maximal Stokes shifts are best suited for parametric conversion. The Stokes shift dependence on the pump wavelength is the weakest near the maximum, hence the wider wavelength band is possible for the pump.

For the fibre (f1), the maximal Stokes shift is 2700 cm^{-1} at the pump wavelength 1.11 μm, which corresponds to the signal wavelength conversion from 854 to 1585 nm. The effective mode area at the pump wavelength is 2.5 μm^2 and the nonlinear coefficient is $\gamma = 67$ (W km)$^{-1}$.

We compared the effective mode areas for the PCFs with a germanosilicate core and a silica core at the similar dispersion characteristics. The dispersion characteristic with a minimal deviation of the Stokes shifts from the PCF with a germanosilicate core (f1) was found, by using GA, for the pure silica fibre (f2) with parameters $\Lambda = 1.74$ μm, $d_1/\Lambda = 0.47, d_2/\Lambda = 0.22$ and $d_3/\Lambda = 0.9$. We did not succeed in obtaining for (f2) an identical to (f1) dispersion shape by varying parameters in two rings. The dispersion curve for (f2) has a lower maximum value and a larger interval between two zeros. Obviously, pure silica PCFs need more rings for varying parameters in comparison with PCFs with a germanosilicate core to obtain the same dispersion profile. For (f2), the effective mode area is 5.7 μm^2 and the nonlinear coefficient is $\gamma = 21.4$ (W km)$^{-1}$ at the pump wavelength of 1.11 μm, which is three times lower than in the PCF with a germanosilicate core (f1).

Figure 7(c) shows the confinement loss in the fibres (f1) and (f2). For the fibre with a germanosilicate core, the losses are significantly lower in the short wavelength region <1.3 μm, even though this fibre has the smaller Λ. In the long wavelength region, losses become too large for both fibres.

Our calculations show that the same dependence of the phasematched Stokes shifts on the pump wavelength can be obtained at different fibre parameters. Figure 8 demonstrates the three dispersion curves, with which the maximal Stokes shift of 2553 cm^{-1} is possible at a pump wavelength of 1.11 μm. The curves were obtained with $d_{GeO_2} = 1.2$ μm by varying Λ, d_1 and d_2. The dispersion curves with smaller Λ have a smaller effective mode area, but a higher confinement loss. As was seen from figure 8(c), the sharp increase of losses in the region of 1.5 μm occurs even for fibre (f1) with a large hole-to-pitch value in the second ring $d_2/\Lambda = 0.84$.

Since three-ring PCFs have a large confinement loss for the Stokes radiation in the region of 1.5 μm, we studied the influence of the fourth ring with a large value of d_4/Λ on the dispersion and waveguide characteristics. The typical result is shown in figure 8 for the fibre (f1), for which the smallest effective area $A_{eff} = 1.78$ μm^2 corresponding to $\gamma = 94$ (W km)$^{-1}$ was found. The addition of the fourth ring with $d_4/\Lambda = 0.9$ had no noticeable effect on the dispersion characteristic up to the wavelength region of 1.6 μm, but essentially (by three orders of magnitude) decreased the confinement loss. According to our estimates made at fixed structural parameters along the fibre, the PCF with $d_4/\Lambda = 0.9$ and with the other parameters identical to those of fibre (f1) allows parametric wavelength conversion of the signal from 866 to 1552 nm with amplification of 10 dB at the pump power of 1 W at 1.11 μm and the fibre length of 20 m.

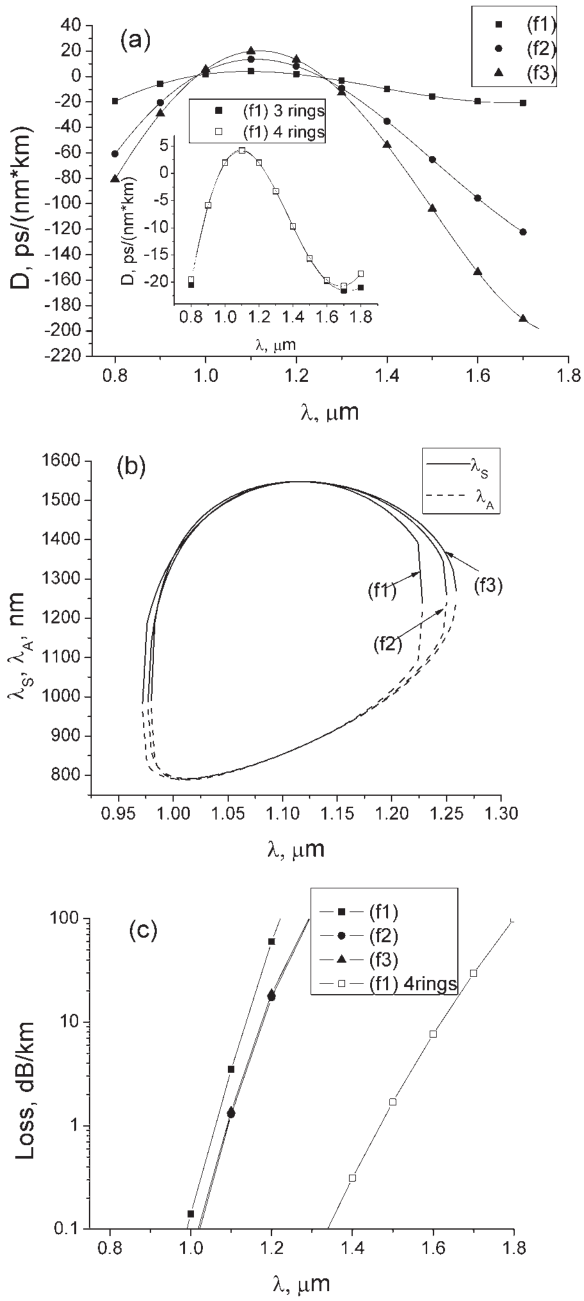

Figure 8. The dispersion (a), the Stokes shifts (b) and the confinement loss (c) for three-ring fibres with the same value for maximum Stokes shifts. (f1) $\Lambda = 1$ μm,$d_{GeO_2} = 1.2$ μm, $d_1/\Lambda = 0.415, d_2/\Lambda = 0.84$ and $d_3/\Lambda = 0.9$; (f2) $\Lambda = 1.35$ μm, $d_{GeO_2} = 1.2$ μm, $d_1/\Lambda = 0.5, d_2/\Lambda = 0.4$ and $d_3/\Lambda = 0.9$; (f3) $\Lambda = 1.5$ μm, $d_{GeO_2} = 1.2$ μm, $d_1/\Lambda = 0.54, d_2/\Lambda = 0.19$ and $d_3/\Lambda = 0.9$. The dispersion and the confinement loss for the four-ring fibre with $d_4/\Lambda = 0.9$ in the fourth ring and with parameters in the first three rings identical to those of fibre (f1) are shown in the inset of (a) and in (c), respectively.

5. Conclusion

In conclusion, we have demonstrated numerically that in a technologically simple design of two-ring PCFs with equal holes, the germanosilicate core significantly extends the possibility of controlling dispersion and nonlinear characteristics. In particular, in the zero wavelength region of 1.1 μm, nonlinear coefficients of 40 (W km)$^{-1}$ and 97 (W km)$^{-1}$ can be achieved in a PCF with 24 mol% GeO_2 and 50 mol% GeO_2, respectively. These γ values appear to be unachievable in pure silica PCFs with the same design of the holes.

In the second type of three-or four-ring PCFs with unequal hole diameters in different rings, we performed an optimization of the dispersion curves with two zeros with the aim to realize FWM with Stokes shifts of 2000–3000 cm^{-1} in the anomalous dispersion region. Nonlinear coefficient $\gamma = 94$ (W km)$^{-1}$ can be achieved for an optimized dispersion in a PCF with 24 mol% GeO_2-doped core. The germanosilicate core was shown to reduce an effective mode area and number of rings with the parameters varying for obtaining the necessary dispersion shape. A more than threefold increase of γ is expected for the same phasematched Stokes–anti-Stokes diagram in a fibre with the 24 mol% GeO_2-doped core as compared to the pure silica core fibre of the same design. However, the presence of a germanosilicate core in a three-ring fibre does not lead to a significant decrease in the confinement loss in the Stokes wavelength region of 1.5 μm. For reducing losses to ~1 dB km^{-1} for wavelengths longer than 1.2 μm, a fourth ring with a large hole-to-pitch ratio d_4/Λ should be added.

For both of the PCFs types with the 24 mol% GeO_2-doped core, the possibility of efficient parametric conversion with Stokes frequency shifts of 2000–3000 cm^{-1} at continuous pump powers in the region of 1.1 μm with fibre lengths of only 20–50 m was shown.

References

[1] Mogilevtsev D, Birks T A and Russel P St J 1998 *Opt. Lett.* **23** 1662

[2] Ranka J K, Windeler R S and Stenz A J 2000 *Opt. Lett.* **25** 25

[3] Knight J C, Arriaga J, Birks T A, Ortigossa-Blanch A, Wadsworth W J and Russel P St J 2000 *IEEE Photon. Technol. Lett.* **12** 807

[4] Renversez G, Kuhlmev B and McPhedran R 2003 *Opt. Lett.* **28** 989

[5] Poli F, Cucinotta A, Selleri S and Bouk A H 2004 *IEEE Photon. Technol. Lett.* **16** 1065

[6] Reeves W H, Knight J C, Russel P St J and Roberts P J 2002 *Opt. Express* **10** 609

[7] Saitoh K, Koshiba M, Hasegawa T and Sasaoka E 2003 *Opt. Express* **11** 843

[8] Andersen T V, Hilligsøe K M, Nielsen C K, Thøgersen J, Hansen K P, Keiding S R and Larsen J J 2004 *Opt. Express* **12** 4113

[9] Karlsson M 1998 *J. Opt. Soc. Am.* B **15** 2269

[10] Monro T M, Richardson D J, Broderick N G R and Bennett P J 1999 *J. Lightwave Technol.* **17** 1093

[11] Hansen P 2006 *Opt. Express* **11** 1503

[12] Agraval G P 1989 *Nonlinear Fiber Optics* (San Diego, CA: Academic)

[13] Wadsworth W J, Joly N, Knight J C, Birks T A, Biancalana F and Russel P St J 2004 *Opt. Express* **12** 299

[14] Viale P, Fevrier S and Gerome F 2005 *Proc. Comsol Multiphysics Conf. (Paris, France, November 2005)* ed J M Petit and J Daluz (Paris: Comsol France) pp 251–5

[15] Ferrarini D, Vincetti L and Zoboli M 2003 *Proc. OFC 2003 (Atlanta, GA, USA, 2003)* (v 2, F15, 23)

[16] Boskovich A, Chernikov S V, Taylor J R, Gruner-Nielsen L and Levring O A 1996 *Opt. Lett.* **21** 1966

[17] Tse M L V, Horak P, Poletti F, Broderick N G R, Price J H V, Hayes J R and Richardson D J 2006 *Opt. Express* **14** 4445

[18] Kerrinckx E, Bigot L, Douay M and Quiquempois Y 2004 *Opt. Express* **12** 1990

[19] Poletti F, Finazzi V, Monro T M, Broderick N G R, Tse V and Richardson D J 2005 *Opt. Express* **13** 3728